



## Article

# Lack of Autophagy Induction by Lithium Decreases Neuroprotective Effects in the Striatum of Aged Rats

Angelica Jardim Costa<sup>1</sup>, Adolfo Garcia Erustes<sup>1</sup>, Rita Sinigaglia<sup>2</sup>, Carlos Eduardo Neves Girardi<sup>3</sup>, Gustavo José da Silva Pereira<sup>1</sup> , Rodrigo Portes Ureshino<sup>4,5,\*</sup> and Soraya Soubhi Smaili<sup>1</sup>

<sup>1</sup> Department of Pharmacology, Universidade Federal de São Paulo, São Paulo-SP 04044-020, Brazil; angelicajardimcosta@gmail.com (A.J.C.); adolfo.erustes@gmail.com (A.G.E.); gustavo.pereira@unifesp.br (G.J.d.S.P.); ssmaili@unifesp.br (S.S.S.)

<sup>2</sup> Electron Microscopy Centre, Universidade Federal de São Paulo, São Paulo-SP 04023-060, Brazil; rita.sinigaglia@unifesp.br

<sup>3</sup> Department of Psychobiology, Universidade Federal de São Paulo, São Paulo-SP 04023-062, Brazil; carlosnevesgirardi@gmail.com

<sup>4</sup> Department of Biological Sciences, Universidade Federal de São Paulo, Diadema-SP 09913-030, Brazil

<sup>5</sup> Laboratory of Molecular and Translational Endocrinology, Escola Paulista de Medicina, Universidade Federal de São Paulo, São Paulo-SP 04039-032, Brazil

\* Correspondence: rpureshino@gmail.com; Tel.: +55-115-576-4848 (ext. 1045)

**Abstract:** The pharmacological modulation of autophagy is considered a promising neuroprotective strategy. While it has been postulated that lithium regulates this cellular process, the age-related effects have not been fully elucidated. Here, we evaluated lithium-mediated neuroprotective effects in young and aged striatum. After determining the optimal experimental conditions for inducing autophagy in loco with lithium carbonate ( $\text{Li}_2\text{CO}_3$ ), we measured cell viability, reactive oxygen species (ROS) generation and oxygen consumption with rat brain striatal slices from young and aged animals. In the young striatum,  $\text{Li}_2\text{CO}_3$  increased tissue viability and decreased ROS generation. These positive effects were accompanied by enhanced levels of LC3-II, LAMP 1, Ambra 1 and Beclin-1 expression. In the aged striatum,  $\text{Li}_2\text{CO}_3$  reduced the autophagic flux and increased the basal oxygen consumption rate. Ultrastructural changes in the striatum of aged rats that consumed  $\text{Li}_2\text{CO}_3$  for 30 days included electrondense mitochondria with disarranged cristae and reduced normal mitochondria and lysosomes area. Our data show that the striatum from younger animals benefits from lithium-mediated neuroprotection, while the striatum of older rats does not. These findings should be considered when developing neuroprotective strategies involving the induction of autophagy in aging.

**Keywords:** aging; autophagy; lithium; striatum; mitochondria; lysosome



**Citation:** Costa, A.J.; Erustes, A.G.; Sinigaglia, R.; Girardi, C.E.N.; Pereira, G.J.d.S.; Ureshino, R.P.; Smaili, S.S. Lack of Autophagy Induction by Lithium Decreases Neuroprotective Effects in the Striatum of Aged Rats. *Pharmaceutics* **2021**, *13*, 135. <https://doi.org/10.3390/pharmaceutics13020135>

Academic Editor: Yulia Sidorova  
Received: 10 November 2020  
Accepted: 18 January 2021  
Published: 21 January 2021

**Publisher's Note:** MDPI stays neutral with regard to jurisdictional claims in published maps and institutional affiliations.



**Copyright:** © 2021 by the authors. Licensee MDPI, Basel, Switzerland. This article is an open access article distributed under the terms and conditions of the Creative Commons Attribution (CC BY) license (<https://creativecommons.org/licenses/by/4.0/>).

## 1. Introduction

There is a progressive loss of cellular homeostasis during aging, accompanied by a reduction in the progenitor cell reserve. These results were seen in many senescent cells that present organellar defects, ultimately leading to a gradual decline in function during aging [1,2]. The cells of the central nervous system (CNS), including the striatal neurons, are especially vulnerable to cell death during aging. Previous studies have associated this enhanced vulnerability to elevated reactive oxygen species (ROS) levels, reduced mitochondrial membrane potential ( $\Psi_m$ ), increased pro-apoptotic Bax and/or reduced anti-apoptotic Bcl-2 protein expression [3,4].

Additionally, one of the most critical regulators of cell homeostasis is autophagy, which plays a vital role in longevity in several experimental models [5–8]. Autophagy is a highly regulated catabolic process that generally participates in cellular viability mechanisms under stress conditions, such as nutrient deprivation, hypoxia, endoplasmic reticulum stress, DNA damage, among others [9,10]. This process contributes to the renewal of cellular

components related to dysfunctional organelles, macromolecules, long-lived and misfolded proteins, toxins and parasites [11,12]. The macroautophagy herein referred to as autophagy involves the formation of autophagosomes with a double-membrane structure, which fuses with lysosomes to form the autophagolysosomes where the cargo is degraded and recycled [11,13,14].

While numerous studies have associated age-related cellular homeostasis dysregulation with autophagy defects, it remains unclear how this catabolic process is modulated throughout life. It has been postulated that the accumulation of undigested material in the lysosomes (lipofuscin) and secondary lysosomes (e.g., autolysosomes) during aging could interfere with autophagosome fusion and cargo degradation, eventually leading to cell death [15] and favoring the pathogenesis of neurodegenerative processes [16,17]. In this context, the pharmacological modulation of autophagy represents a potential therapy for age-related diseases. Indeed, rapamycin [18], clonidine [19] and trehalose [20] have been shown to provide autophagy-mediated neuroprotection. Furthermore, Harrison et al. (2009) demonstrated that rapamycin increases the life expectancy of male mice by 9% and females by 14% [21].

Over the last twenty years, a growing amount of evidence shows that lithium could be used to treat neurodegenerative disorders [22–26]. For example, Sarkar et al. demonstrated that lithium induces autophagy, independently of mTOR, by inhibiting inositol monophosphatase (IMPase), resulting in the clearance of huntingtin and  $\alpha$ -synuclein in non-neuronal and neural precursor cells [27]. On the other hand, studies have reported that lithium is a direct [28,29] and indirect [30,31] negative regulator of GSK3- $\beta$ , contributing to autophagy inhibition by activating mTOR [32]; thus, an imbalance of these pathways can affect autophagy regulation. Since few reports have explored the modulation of autophagy in the aging striatum [33–35], the present study sought to evaluate the effects of lithium treatment on this brain structure in young and aged animals, which is particularly relevant to neurodegeneration.

## 2. Materials and Methods

### 2.1. Animals

The experiments were performed with two groups of Wistar 2BAW rats, young (4–6 months-old) and aged (24–26 months-old). The sample size ( $n = 2-4$ ) was determined based on the reproducibility of the results and considering the challenges of keeping aged animals for the proposed work. It is important to point out that during the process of aging, 2/3 of the animals died and only the animals that reached the age of 24–26 months were considered. All the samples and biologic materials available were studied, where a maximum number of images and parameters were acquired and measured. Thus, this provided reproducible and unique results in terms of aging studies. Throughout the experimental period, the animals were maintained in the Institute of Pharmacology and Molecular Biology animal facility at the Federal University of São Paulo, under controlled light (12 h light–dark cycle) and temperature ( $23 \pm 2$  °C) conditions to assure the quality control and the accuracy of the experiments. The rats consumed standard rat chow and water ad libitum. All the procedures performed in this study were approved by and are in accordance with the ethical standards of the Institutional Ethics Committee (CEUA/UNIFESP 1907220814).

### 2.2. Acute and in Loco Treatments in Striatal Slices

#### 2.2.1. Brain Slices Preparation and Lithium Treatments

Tissue collection involved euthanizing the animals by decapitation, gently opening the skulls, and quickly removing the whole brain. Each brain was then gently sliced with a vibratome. The subsequent coronal sections containing the frontal cortex, corpus callosum and striatum triad of approximately 400  $\mu\text{m}$  were immersed in an artificial cerebral–spinal fluid (aCSF) solution supplemented with sucrose (2 mM KCl, 1 mM  $\text{CaCl}_2$ , 26 mM  $\text{NaHCO}_3$ , 1.25 mM  $\text{NaH}_2\text{PO}_4$ , 1 mM  $\text{MgCl}_2$ , 2 mM  $\text{MgSO}_4$ , 10 mM glucose, sucrose

248 mM, pH 7.4). Then the slices were incubated in maintenance aCSF solution (2 mM KCl, 2 mM CaCl<sub>2</sub>, 26 mM NaHCO<sub>3</sub>, 1.25 mM NaH<sub>2</sub>PO<sub>4</sub>, 2 mM MgSO<sub>4</sub>, 10 mM glucose, 124 mM NaCl, pH 7.4) [4]. The solution was constantly aerated with a perfusion pump and maintained at room temperature (20–25 °C). The slices were kept under these conditions for at least 45 min for tissue stabilization and then treated with lithium carbonate (Li<sub>2</sub>CO<sub>3</sub>, at concentrations of 0.1, 1 or 10 mM) in the presence or absence of ammonium chloride (NH<sub>4</sub>Cl). In all experiments the untreated striatal slices of either young (4–6 months-old) or aged (24–26 months-old) animals were used as controls.

### 2.2.2. Western Blotting Analysis

Coronal sections of the striatum were dissected and homogenized in radioimmuno-precipitation assay (RIPA) buffer (150 mM NaCl, 1% NP-40, 0.5% sodium deoxycholate, 0.1% SDS, 50 mM Tris-HCl, 2 mM MgCl<sub>2</sub>) supplemented with protease inhibitors (Phenylmethylsulfonyl fluoride—PMSF and Protease Inhibitors Cocktail). The homogenate was sonicated and centrifuged at 5000 rpm for 30 min at 4 °C to remove the cellular debris, and the supernatant fraction was collected. An aliquot of the supernatant corresponding to 50 µg of total protein was subjected to thermal denaturation (95 °C for 10 min) in sample buffer (12% SDS, 40% glycerol, 120 mM ethylenediaminetetraacetic acid (EDTA), 1 mg/mL bromophenol blue, 375 mM Tris/HCl, pH 6.8). The protein samples were then separated by SDS-PAGE and subsequently transferred to a polyvinylidene difluoride (PVDF) membrane (Merck Millipore, Burlington, MA, USA). The membranes were probed with the following primary antibodies: rabbit polyclonal anti-Ambra 1 (1:200, Merck Millipore, Burlington, MA, USA, Cat# ABC131), rabbit monoclonal anti-beclin-1 (1:1000, Cell Signaling Technology, Danvers, MA, USA, Cat# 3738), rabbit monoclonal anti-LC3B (1:1000, Cell Signaling Technology, Cat# 2775), rabbit monoclonal anti-p-GSK-3β (1:500, Cell Signaling Technology, Cat# 9336), rabbit monoclonal anti-GSK-3β (1:1000, Cell Signaling Technology, Cat# 9581), rabbit monoclonal anti-LAMP1 (1:500; Santa Cruz Biotechnology Inc, Dallas, TX, USA, Cat# sc-20011) and, as an internal control, rabbit polyclonal anti-β-actin (1:1000; Sigma-Aldrich, St. Louis, MO, USA, Cat# A5060). After overnight incubation, the membranes were washed and then incubated with the appropriate Horseradish Peroxidase-conjugated secondary antibodies, goat polyclonal anti-rabbit (1:5000; Thermo Fisher Scientific, Waltham, MA, USA, Cat# 31460) and goat polyclonal anti-mouse (1:5000; Thermo Fisher Scientific, Cat# G-21040). The Western blots were developed with enhanced chemiluminescent reagent (PerkinElmer, Waltham, MA, USA) and the immunoreactive bands were visualized using a high-resolution photo documentation system (UVITEC Alliance 4.7, Cambridge, UK). The semiquantitative analysis was performed by densitometry evaluating optical intensity of the immunoreactive protein bands using the Alliance software (UVITEC, Cambridge, UK). The intensity of the bands was normalized in relation to the β-actin band. All data were expressed as a percentage of the young control group (100%).

### 2.2.3. Cell Viability and ROS Measurements

The cell viability and ROS generation assays were performed in a multi-mode microplate reader (FlexStation 3, Molecular Devices, San Jose, CA, USA) operating in the fluorescence mode. The fluorescence data were extracted using the SoftMax Pro 7 software (Molecular Devices).

For the cell viability assay, the lithium-treated and untreated brain slices of young and aged rats were loaded with 10 µM Calcein-AM (excitation/emission: 488/525 nm) plus 0.01% Pluronic F-127 for 30 min at 37 °C. Calcein-AM, when crossing the cell membrane, is cleaved by esterases of viable cells producing a fluorescent compound. The fluorescence intensity was recorded, and the maximum fluorescence was used for the analyses.

For the measurements of ROS generation, the lithium-treated and untreated brain slices of young and aged rats were incubated with 5 µM CM-H<sub>2</sub>DFCDA (“5-(and-6)-chloromethyl-2',7'-dichlorodihydro fluorescein diacetate, acetyl ester”) indicator (ex./em. 488/525 nm) for 30 min at 37 °C. CM-H<sub>2</sub>DFCDA in the presence of reactive species is

oxidized to 2',7'-dichlorofluorescein (DCF), a highly fluorescent product. Initially, a baseline was recorded for 2 min, and then the slices were stimulated with 1 mM glutamate. Metabotropic and ionotropic receptor stimulation by glutamate leads to an increase in cytoplasmic  $\text{Ca}^{2+}$  level, which can activate the electron transport chain and increase  $\Delta\Psi_m$  and ROS generation [36]. The tissues were then treated with 60 mM tert-butyl hydroperoxide (TBHP), which produces the maximum fluorescence ( $F_{\text{max}}$ ) by promoting an increase in ROS production that oxidizes all of the intracellular DCF. The values were normalized to the baseline fluorescence and expressed as percentages of the maximum fluorescence ( $F_{\text{max}} = 100\%$ ).

#### 2.2.4. Oxygen Consumption Rate Measurement

The coronal brain slices were treated with lithium as described above, and then oxygen consumption was measured. Striatal slices were isolated to assess the mitochondrial respiration rate using an oxygraph system (OXYG2, Hansatech Instruments, Leicester, UK). Each striatal slice was immersed in the oxygraph chamber containing aCSF and maintained at 37 °C. The baseline oxygen consumption values were recorded for 2.5 min, followed by the addition of adenosine diphosphate (ADP, 5  $\mu\text{M}$ ) and inorganic phosphate ( $\text{Na}_2\text{HPO}_4$ , 5  $\mu\text{M}$ ). These substrates were used to stimulate mitochondrial respiration state 3, with a subsequent increase in oxygen, which should return to the basal state, state 4, after approximately 5 min. The oxygen consumption was expressed as a linear regression function of its concentration over time. The rate of state 3/4 was considered as the ADP:O ratio ( $\text{O}_2$  consumption rate per ADP molecule consumed). Basal oxygen consumption was established by state 4 measures and data expressed as a percentage of the young control samples (100%).

#### 2.3. Chronic and In Vivo Treatment and Ultrastructural Analysis

For the ultrastructural analysis of the striatum, two animals from each group were treated with  $\text{Li}_2\text{CO}_3$  in the drinking water (4.7 mM) given ad libitum for 30 days. After treatment, all animals were anesthetized with halothane, intubated and connected to a mechanical respirator. The animals were then transcardially perfused with phosphate-buffered saline (PBS) solution containing 2.5% glutaraldehyde and 2.0% formaldehyde at a continuous flow of 15 mL/min using a perfusion pump (Easy-load model 7518-60, Masterflex pump controller, Cole Parmer, Vernon Hills, IL, USA). After euthanizing, the brains were gently removed and left overnight in the same fixative. The brains were coronally cutted at 1 mm-thick. One section from the dorsolateral region of the striatum (1.8 mm from bregma, Paxinos) was trimmed for obtaining a 1-mm<sup>3</sup> sample. The samples were washed in 0.1 M cacodylate buffer and post-fixed in 2% osmium tetroxide/3% potassium ferrocyanide (30 min), contrasted in uranyl acetate, dehydrated in alcohol, cleared in propylene oxide and embedded in Epon resin. Semi-thin sections (500 nm thick) were obtained using an ultramicrotome (Ultracut R, Leica, Wetzlar, Germany) and stained with toluidine blue alcoholic solution. These semi-thin sections were examined under a light microscope (Olympus BX41) to select the optimal area to be observed in a transmission electron microscope. We then obtained ultrathin sections (70 nm thick) using an ultramicrotome (Ultracut R, Leica). These sections were collected in copper mesh, contrasted with uranyl acetate and lead citrate, and subsequently examined with a transmission electron microscope (1200 EXII, JEOL). Electron micrographs were obtained with a Multiscan 791 digital camera (GATAN, Pleasanton, CA, USA), and the obtained images were analyzed with the ImageJ software (1.46r, NIH, Bethesda, MD, USA).

#### 2.4. Statistical Analyses

All values are represented as the mean  $\pm$  standard error of the mean (SEM). Comparisons between two means were determined using the unpaired Student's *t* test. Between group comparisons (three or more means) were performed using one-way ANOVA followed by Dunnett's post-hoc test and two-way ANOVA followed by Bonferroni's post-hoc

test using the GraphPad Prism 5 software. Differences were considered statically significant when  $p < 0.05$ .

### 3. Results

#### 3.1. Acute Lithium Treatment Promotes Opposite Effects on Autophagy in Young and Aged Rat Striatum

Before comparing the effects of lithium on young and aged striatal slices, we first determined the concentration and exposure time required for inducing autophagy in the young samples, as evidenced by an increase in LC3-II expression. As shown in Figure 1a, striatal slices from young rats were treated in loco with three different concentrations of  $\text{Li}_2\text{CO}_3$  (0.1 mM, 1 mM and 10 mM) for 1.5 h or 3 h. We found that 0.1 mM of  $\text{Li}_2\text{CO}_3$  for 1.5 h induced an increase in LC3-II levels compared to the untreated control slices. Notably, this effect was no longer evident after 3 h. Since lithium appeared to be a potential autophagic inducer, we then evaluated the effect of treating striatal slices from aged rats with 0.1 mM of  $\text{Li}_2\text{CO}_3$  for 1.5 h.

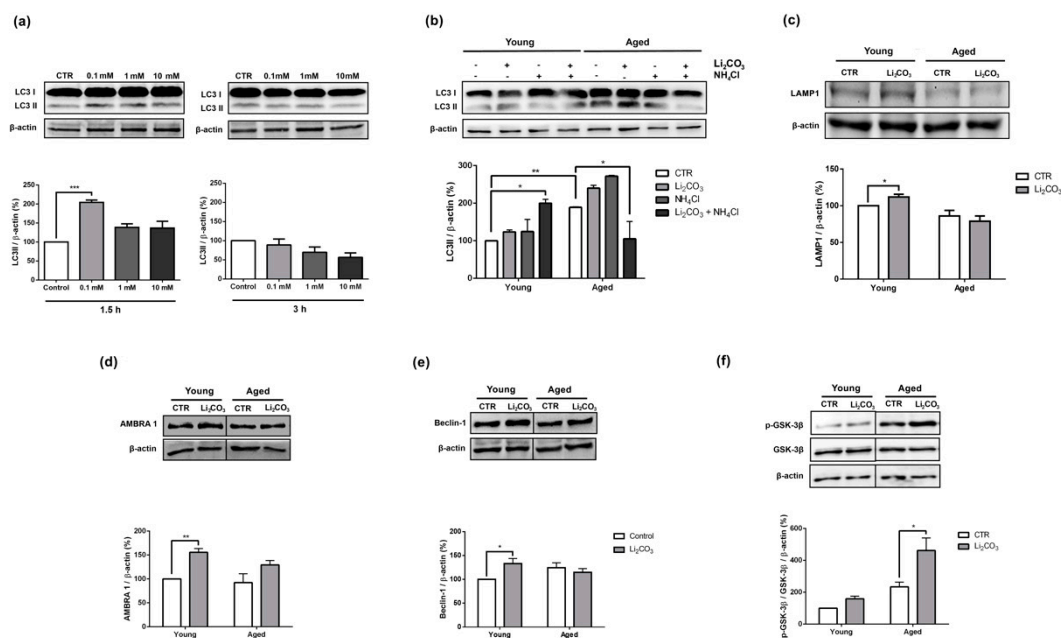


**Figure 1.** Lithium blocked autophagy in striatal slices of aged rats, possibly by GSK-3 $\beta$  inhibition. (a) Young animals striatal slices were treated with several concentrations (0.1, 1 and 10 mM) of  $\text{Li}_2\text{CO}_3$  for 1.5 h and 3 h, and the LC3-II expression was detected by Western blotting. (b) LC3-II expression levels were detected by Western blotting after 1.5 h of 0.1 mM  $\text{Li}_2\text{CO}_3$  treatment in the presence or absence of  $\text{NH}_4\text{Cl}$  (4 mM) in young and aged animals. (c) LAMP 1, (d) Ambra 1, (e) Beclin-1, (f) p-GSK-3 $\beta$  (Ser 9) and GSK-3 $\beta$  expressions levels were detected by Western blotting after 1.5 h of 0.1 mM  $\text{Li}_2\text{CO}_3$  treatment in striatal slices of young and aged animals. Representative Western blot autoradiographies are shown on the top panels and the histograms showing mean  $\pm$  standard error of the mean (SEM) of bands' relative density are shown on the bottom panels. All values were normalized to  $\beta$ -actin and expressed as percentages of the control young animals (100%) ( $n = 2-4$ ). (a) \*  $p < 0.05$  compared to control (one-way ANOVA, Dunnet post-hoc); (b,d-f) \*  $p < 0.05$  or \*\*  $p < 0.01$  compared to control (one-way ANOVA, Bonferroni post-hoc); (c) \*  $p < 0.05$  compared to control (Student's  $t$ -test).

Then, we evaluated LC3-II levels in striatal slices from young and aged rats treated in loco with 0.1 mM of  $\text{Li}_2\text{CO}_3$  for 1.5 h in the presence (added in the last hour of the  $\text{Li}_2\text{CO}_3$  treatment) or absence of 4 mM ammonium chloride ( $\text{NH}_4\text{Cl}$ ). This weak base is protonated in acidic organelles and inhibits the terminal stages of autophagy. This methodology provides invaluable information about the kinetics of the system and cargo clearance, assessing LC3 II turnover [37]. Figure 1b shows that the striatal slices from the aged rats presented significantly higher basal levels LC3-II than the young control slices. In the striatal slices from young rats,  $\text{Li}_2\text{CO}_3$  induced the complete autophagic flux, and

$\text{Li}_2\text{CO}_3 + \text{NH}_4\text{Cl}$  resulted in a nearly two-fold increase in LC3-II levels compared to  $\text{Li}_2\text{CO}_3$  alone. On the other hand, striatal slices from aged rats treated with  $\text{Li}_2\text{CO}_3 + \text{NH}_4\text{Cl}$  exhibited a significant decrease in the levels of LC3-II, a result that suggests that autophagy might be impaired in the aged animals (Figure 1b).

LAMP1 expression was also assessed in striatal slices of young and aged animals treated with  $\text{Li}_2\text{CO}_3$  for 1.5 h. LAMP 1 is a structural protein of the lysosome/late endosome that can be used as another indicator for autophagic flux modulation [37]. The results showed that treatment with  $\text{Li}_2\text{CO}_3$  increased the expression of LAMP 1 in young animals. Furthermore, it is possible to observe a reduction in the LAMP 1 expression of aged animals compared to the young control group, although no statistical significance was detected (Young CTR vs Aged CTR  $p$  value = 0.1394) (Figure 1c).

Since the induction of autophagy is mainly regulated by the Beclin 1 complex, which interacts with several cofactors such as Ambra 1 (activating molecule in Beclin-1-regulated autophagy) [38], we investigated the effects of  $\text{Li}_2\text{CO}_3$  treatment on Ambra 1 and Beclin-1 expression levels (Figure 1d,e) in the striatum of young and aged rats. In the young animal slices treated with  $\text{Li}_2\text{CO}_3$ , the levels of both Ambra 1 and Beclin-1 were significantly increased when compared to the young control group. While a similar trend was also observed in the striatal slices of aged rats treated with  $\text{Li}_2\text{CO}_3$ , these values failed to reach a level of significance and thus indicate no modulation in the levels of these autophagy-inducer phase proteins (Figure 1d,e). Next, we evaluated the effect of  $\text{Li}_2\text{CO}_3$  treatment on glycogen synthase kinase  $3\beta$  phosphorylation. For this, we utilized an antibody that specifically reacts with the inactive form of GSK- $3\beta$  phosphorylated at serine 9 (p-GSK- $3\beta$ , a posttranslational modification related to the mTORC1 inactivation and autophagy induction). Here we observed that the expression levels of p-GSK- $3\beta$  were significantly increased in brain slices of aged rat treated with  $\text{Li}_2\text{CO}_3$  (Figure 1f). This result suggests that inhibition of the GSK- $3\beta$  pathway may be involved in autophagy blockage in older animals.

### 3.2. Acute Lithium Treatment Exerts an Age-Dependent Effect on Cell Viability and ROS Generation

After assessing the effect of  $\text{Li}_2\text{CO}_3$  on autophagy induction, we then decided to focus our attention on the possible role this ion has in cytoprotection. Towards this goal, we evaluated the effects of  $\text{Li}_2\text{CO}_3$  on cell viability (Figure 2a) and ROS generation (Figure 2b) in the striatum from young and aged rats by measuring the maximal fluorescence emitted from Calcein-AM and CM- $\text{H}_2\text{DFCDA}$ , respectively. As shown in Figure 2a, the  $\text{Li}_2\text{CO}_3$ -treated striatal slices from the young rats exhibited significantly higher fluorescence intensities, indicating enhanced cell viability compared to untreated control slices. In contrast,  $\text{Li}_2\text{CO}_3$  did not affect the cell viability of the striatal slices from aged animals (Figure 2a).

The quantification of the CM- $\text{H}_2\text{DFCDA}$  fluorescence, following glutamate stimulation, demonstrated that  $\text{Li}_2\text{CO}_3$  attenuates ROS production in the striatal slices of young rats when compared to untreated control slices. On the other hand,  $\text{Li}_2\text{CO}_3$  afforded no protection against the glutamate-induced ROS generation in the brain slices from aged animals (Figure 2b).

### 3.3. Acute Lithium Treatment Increases $\text{O}_2$ Consumption

The mitochondrial respiratory function was assessed by measuring the ADP:O ratios and basal  $\text{O}_2$  consumption rates in the striatum slices of young and aged animals treated with 0.1 mM  $\text{Li}_2\text{CO}_3$  for 1.5 h. We observed that the untreated control brain slices from the young rats presented a significantly higher ADP:O ratio than aged control slices. Interestingly, young striatal slices treated with  $\text{Li}_2\text{CO}_3$  displayed a significantly reduced ADP:O ratio comparable to the ratios observed in the untreated and  $\text{Li}_2\text{CO}_3$ -treated slices from aged animals (Figure 2c, bar graph, lower left). Concerning the basal rate of  $\text{O}_2$  consumption, a significantly higher value was observed in the aged striatal slices treated with  $\text{Li}_2\text{CO}_3$ , suggesting that mitochondrial respiration is modulated under these conditions (Figure 2c, bar graph, lower right).

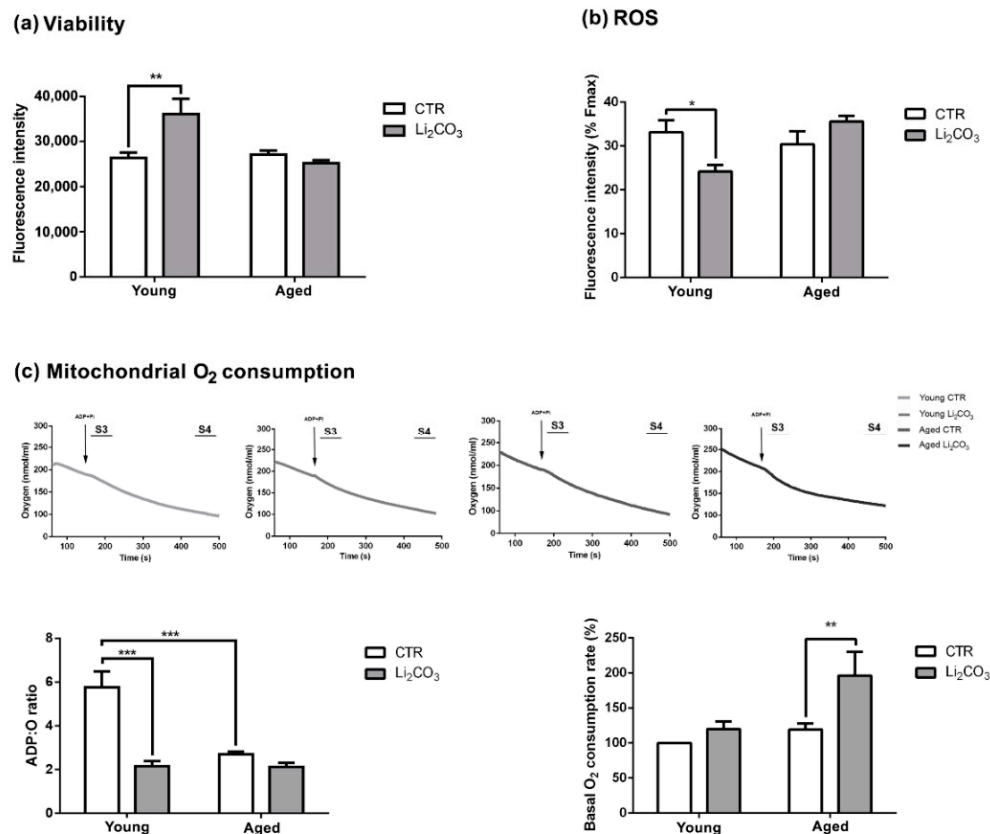


**Figure 2.** Cytoprotective effect of lithium in young but not aged striatal slices. Histograms of the mean maximum fluorescence of (a) calcein in the striatum of young and aged rats, (b) 5-(and-6-)chloromethyl-2',7'-dichlorodihydrofluorescein diacetate, acetyl ester (CM-H<sub>2</sub>DFCDA) after stimulus with glutamate (1mM) and normalized by tert-butyl hydroperoxide (TBHP) (30 mM); (c) Histogram of the adenosine diphosphate (ADP):O ratio (state 3/4) after the addition of adenosine diphosphate (ADP, 5  $\mu$ M) and inorganic phosphate (Na<sub>2</sub>HPO<sub>4</sub>, 5  $\mu$ M) and basal oxygen consumption rate analyzed by state 4 measures. The values are presented as a ratio or percentage of consumption oxygen rate (b,c). All histograms are a mean  $\pm$  SEM ( $n = 4$ ). \*  $p < 0.05$ , \*\*  $p < 0.01$  and \*\*\*  $p < 0.001$  compared to control (two-way ANOVA, Bonferroni post-hoc).

### 3.4. Chronic Lithium Treatment Increases Organelle Damage in Aged Striatum

To determine if lithium induces ultrastructural changes in the striatum, we administered Li<sub>2</sub>CO<sub>3</sub> to young and aged animals for 30 days. The consumption of lithium solution (4,7 mM Li<sub>2</sub>CO<sub>3</sub>, dissolved in drinking water—which corresponds to 0.35 mg/mL) was monitored during the 30 days of treatment to obtain an average dose administered per animal. The young animals consumed an average of  $20 \pm 3.7$  mL/day of Li<sub>2</sub>CO<sub>3</sub> solution, and considering the animal weight of approximately  $208.8 \pm 8.5$  g, it corresponds to  $\approx 34$  mg/kg. Likewise, the aged animals consumed  $24.8 \pm 6.9$  mL/day of Li<sub>2</sub>CO<sub>3</sub> solution and presented an average weight of  $222.6 \pm 34.9$  g, resulting in a calculated dose of  $\approx 38$  mg/kg. Therefore, an average of 4 mg/kg more was administered to the aged animals; however, considering that the weight and lithium consumption of aged animals are less homogenous than in the young, this difference does not represent a significant mean variation in lithium uptake between groups.

In Figure 3a, the striatum from young untreated control animals exhibits the typical ultrastructural features of medium spiny neurons [39], a typical area of mitochondria (Figure 3e) and a small number of lysosomes (Figure 3g). In contrast, there were significantly more normal and total mitochondria area per cytoplasm area (Figure 3e,f) and larger lysosomes, many filled with lipofuscin (telolysosomes) in the untreated control striatum from aged rats (Figure 3c). The representative image of Li<sub>2</sub>CO<sub>3</sub>-treated striatum from a young rat in Figure 3b shows the normal ultrastructural appearance of all organelles and the presence

of autophagic vacuoles (arrow) (Figure 3b). In contrast, total mitochondria and lysosomes area were increased (Figure 3f,g). Treating aged striatum with  $\text{Li}_2\text{CO}_3$  caused alterations in mitochondria, including reduced normal mitochondria area (Figure 3e), swelling and disarranged cristae (Figure 3d). Furthermore, the number and size of the lysosomes were significantly reduced in  $\text{Li}_2\text{CO}_3$ -treated aged striatum (Figure 3d,g), which corroborates our previous findings with the autophagy markers.

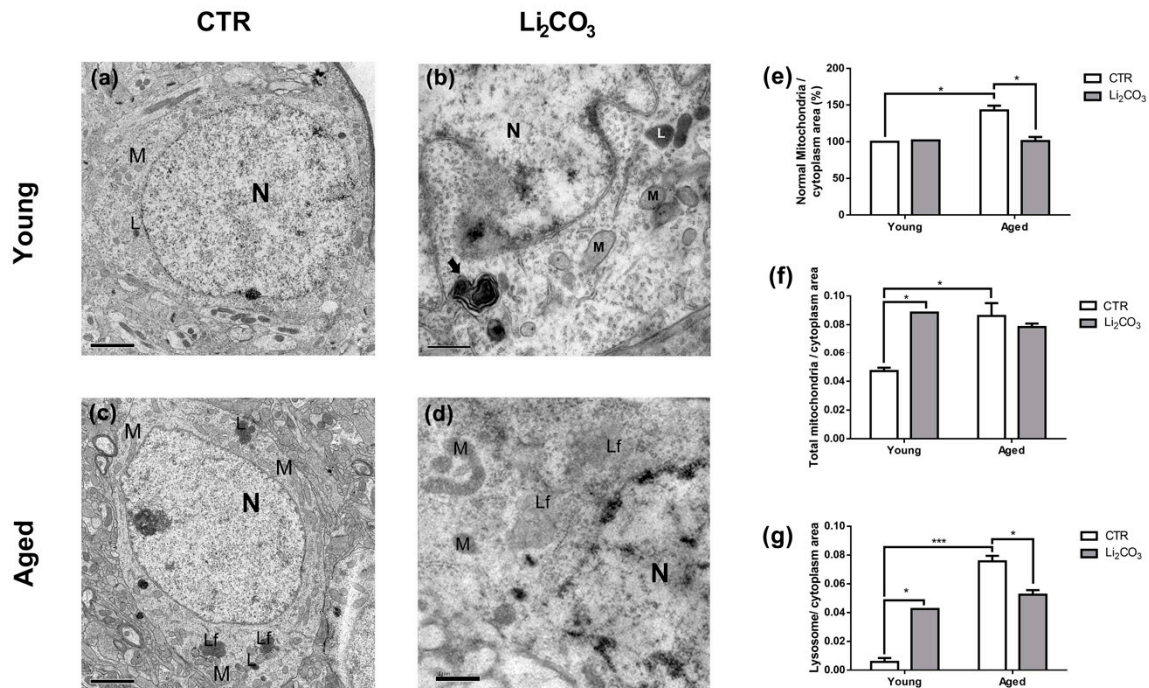


**Figure 3.** Lithium alters the morphology of organelles in the striatum of aged rats. Representative electron micrographs of dorsolateral striatal neurons from young and aged control animals (a) and (c), respectively) or  $\text{Li}_2\text{CO}_3$  treated (4.7 mM, 30 days) young and aged animals (b) and (d), respectively). In (a,c), representative striatal neurons displaying diverse organelles with normal appearances, like mitochondria (M), lysosome (L), telolysosome (lipofuscin granule, Lf) and nucleus (N). In (b), a striatal neuron of a  $\text{Li}_2\text{CO}_3$ -treated young animal showing the normal ultrastructural appearance of all organelles like mitochondria (M), heterolysosome (L), and nucleus (N) and the presence of an autophagic vacuole (arrow). In (d), a striatal neuron of a  $\text{Li}_2\text{CO}_3$ -treated aged animal revealing some telolysosome (lipofuscin granule, Lf) and electrondense mitochondria with swollen cristae (M). Scale bars represent 2  $\mu\text{m}$  in (a) and (b); 1  $\mu\text{m}$  in (c) and (d). Micrographs digitally obtained (Orius GATAN, USA) through a transmission electron microscope at 80 kV (JEOL1200 EXII, Japan). Histograms showing normal (e) and total (f) mitochondria area, and lysosomes (g) in relation to the cytoplasm area. In (e) the values are presented as a percentage of the control. All histograms are a mean  $\pm$  SEM ( $n = 2$ ). \*  $p < 0.05$ , \*\*  $p < 0.01$  and \*\*\*  $p < 0.001$  (two-way ANOVA, Bonferroni post-hoc).

#### 4. Discussion

Several studies have demonstrated that lithium treatment reduces neurodegeneration parameters in experimental models [23,40–48]. However, most studies on the protective actions of lithium were performed with cell lines or young animals. In the present study, we sought to determine if lithium exerts age-dependent effects that could differentially modulate autophagy, a catabolic protective strategy against neurodegenerative diseases. Towards this goal, we evaluated mitochondrial alterations, including morphological changes, ROS generation and oxygen consumption in young and aged striatum treated with lithium.

It is well known that autophagic activity decreases with age, and it has been shown that impaired autophagy contributes to neurodegeneration in mice [17,49]. Here we demonstrated that lithium modulates autophagy in a brain structure which is a target to the neurodegenerative process in an age-dependent manner. For example, we showed that the levels of LC3-II are elevated in aged striatum. However, upon the treatment with a

concentration of  $\text{Li}_2\text{CO}_3$  that induces autophagy, the LC3-II levels drop sharply (Figure 1b). Additionally, LAMP 1 levels were reduced in untreated and treated aged striata (Figure 1c), suggesting that autophagy flux was blocked. This observation agrees with the results reported by Yamamoto et al. in the murine kidney, where they observed higher basal autophagic activity in aged samples. However, when the young and aged animals were submitted to starvation protocol, only the kidneys of the young animals exhibited GFP-LC3B positive puncta [50], providing evidences that autophagic flux was blocked in older animals. Moreover, Liu et al. (2019) detected higher Beclin-1 and LC3-II expression levels in the striatum of aged rats. They also found that regular aerobic exercise regulates the balance between cell death and autophagy [33].

Lithium is commonly used to treat psychiatric disorders, but the precise mechanism of action is a subject of intense debate in the literature. It has been reported that lithium can modulate autophagy, either in an mTOR dependent or independent pathways, by inhibiting IMPase. Moreover, it is well known that lithium inhibits GSK3- $\beta$ , but the role this kinase plays in autophagy is controversial. For example, in the MCF-7 breast cancer cell line, inhibition of GSK-3 $\beta$  increases autophagy by negatively modulating mTORC1 [51]. On the other hand, in neurodegeneration, Sarkar et al., 2008 demonstrated that lithium increased autophagy by inhibiting IMPase, but decreased autophagy by inhibiting GSK-3 $\beta$  [32]. Here, in aged striatum treated with lithium, we observed higher p-GSK-3 $\beta$  phosphorylation levels at an inhibitory site, which resulted in autophagy blockage (Figure 1f).

Additionally, in contrast to the young striatum, the expression of autophagy inducer-phase proteins Ambra 1 and Beclin-1 were unaltered in the aged tissue, reinforcing the idea that autophagy is inhibited, despite the presence of an autophagy inducer. Interestingly, Castillo-Quan et al., 2016 demonstrated that lithium increased the life and health spans in a *Drosophila melanogaster* aging model. The authors proposed that these effects are probably due to GSK-3 $\beta$  pathway inhibition and do not involve autophagy [52].

Previous studies have also shown that the accumulation of insoluble particles known as lipofuscins can obstruct the autophagic system, leading to an autophagy deficiency in the aging CNS [15,53,54]. Indeed, in this work, we demonstrated that striatum from aged animals presented more lysosomes, with many filled with lipofuscin (Figure 3c,g). Surprisingly, chronic  $\text{Li}_2\text{CO}_3$  treatment reduced the area of lysosomes in the age-matched group (Figure 3d,g). Therefore, since the autophagic flux is attenuated in the  $\text{Li}_2\text{CO}_3$ -treated aged striatum (Figure 1b), it is plausible that the lower area of lysosomes and LAMP 1 levels can contribute to dysregulation in autophagy. However, we can not exclude that a decreased number of lysosomes could be associated to a non-apoptotic cell death triggering [55].

On the other hand, lithium in therapeutic formulations is more related to neuronal survival in several animal models of neurodegeneration, including focal cerebral ischemia, 3-NP, quinolinic acid-induced Huntington's disease-like pathogenesis and a Down's syndrome model [23,40–42]. Fabrizi et al., 2014 demonstrated that lithium promoted cell proliferation and survival and protected PC12 cells (pheochromocytoma cell line) against trimethyltin -induced apoptosis [56]. In this sense, our results agree with these findings since  $\text{Li}_2\text{CO}_3$  was able to increase tissue viability in the young striatum (Figure 2a) but not in aged animals. More evidence of lithium-mediated neuroprotection being age-dependent comes from a study using a transgenic Alzheimer's disease model, in which the drug significantly improved neurogenesis and memory in two-month-old animals compared to six-month-old animals [57]. Autophagy inhibition may be involved with these effects in aged animals; however, it may not be the only factor involved since autophagy blockers did not increase cytotoxicity in vitro [55].

Kim et al., 2011 demonstrated the protective effects of lithium in neurons, after the induction of oxidative stress in models of Parkinson's disease, both in vitro (dopaminergic neurons overexpressing the A53T mutant of  $\alpha$ -synuclein) and in vivo (transgenic mice overexpressing the A53T mutant of  $\alpha$ -synuclein) [45]. Our results showed that  $\text{Li}_2\text{CO}_3$  reduced ROS generation in young striatum but failed to elicit this effect in the aged group (Figure 2b). This result suggests a positive correlation with the increased tissue viability

observed in the  $\text{Li}_2\text{CO}_3$ -treated young tissues (Figure 2a). Indeed, previous studies have shown that therapeutic concentrations (0.5–1 mM) of lithium exert neuroprotective effects due to increased protection against oxidative stress [45,58,59]. The increase in the basal  $\text{O}_2$  consumption rate may lead to enhanced ROS production in the samples treated with lithium (Figure 2c).

Remarkable metabolic alterations that are often associated with mitochondrial dysfunction accompany aging [60,61]. Indeed, alterations in glycolytic intermediates and the tricarboxylic acid cycle, which indicate mitochondrial dysfunction, have been observed during aging and in neurodegenerative diseases, such as Alzheimer's [60]. Chen et al. showed that lithium treatment inhibits GSK-3 $\beta$ , reducing the inactivation of pyruvate dehydrogenase E1 (PDH-E1) and consequently increasing basal and maximal mitochondrial respiration [62]. Here we show that aging promotes a reduction in mitochondrial respiration function, as shown by the ADP:O ratio (Figure 2c), which could account for the mitochondrial alterations detected by electron microscopy. In an animal model of Amyotrophic Lateral Sclerosis, Fornai et al., 2008 showed that lithium reduced mitochondrial swelling and increased the number of normal mitochondria [63]. Here we show that chronic  $\text{Li}_2\text{CO}_3$  treatment increased the total mitochondria area in young animals, as well as reduced normal mitochondria area in the striatum of aged animals, suggesting that lithium induces different subcellular alterations during aging. These increases in normal and total mitochondria area observed in aged animals may be related to autophagy/mitophagy inhibition. Previous studies have shown that autophagic inhibitors such as Wortmannin, bafilomycin A<sub>1</sub> and chloroquine increased the mitochondrial mass in glioma and hepatocellular carcinoma cells lines [64,65]. Additionally, a study using aged rabbits (2.5 years old) with heart failure demonstrated an accumulation of proteins from the autophagic signaling cascade (LC3 and p62) and specific mitophagy processes (Parkin) associated with impairment of the mitochondrial fusion–fission process. It thus could increase the mitochondrial mass [66].

Considering all of the results and discussion in the present study, we conclude that  $\text{Li}_2\text{CO}_3$  treatment may benefit younger animals by attenuating ROS production, modulating autophagic activity and augmenting tissue viability. However,  $\text{Li}_2\text{CO}_3$ -treated aged animals did not present these cytoprotective effects, in addition to lithium-mediated autophagy inhibition. Thus, autophagy appears to be an essential factor for neuroprotection in the young striatum. Indeed, our data show that aged animals present autophagy deficiencies that could limit the putative  $\text{Li}_2\text{CO}_3$ -induced actions. We expect that future studies will identify new autophagy-inducing targets that provide neuroprotection in older animals.

**Author Contributions:** Conceptualization, A.J.C., R.P.U. and S.S.S.; methodology, A.J.C., R.S., R.P.U. and S.S.S.; validation, A.J.C., R.P.U. and S.S.S.; formal analysis, A.J.C. and R.S.; investigation, A.J.C.; resources, A.J.C., R.P.U. and S.S.S.; data curation, A.J.C.; writing—original draft preparation, A.J.C. and R.P.U.; writing—review and editing, A.J.C., A.G.E., R.S., C.E.N.G., G.J.d.S.P., R.P.U. and S.S.S.; visualization, A.J.C.; supervision, R.P.U. and S.S.S.; project administration, R.P.U. and S.S.S.; funding acquisition, G.J.d.S.P., R.P.U. and S.S.S. All authors have read and agreed to the published version of the manuscript.

**Funding:** This research was funded by Fundação de Amparo à Pesquisa do Estado de São Paulo (FAPESP-2012/08273-3; 2013/20073-2; 2016/20796-2; 2013/20976-2; 2017/10863-7, 2019/02821-8), Conselho Nacional de Desenvolvimento Científico e Tecnológico (CNPq-163612/2013-7; PVE 401236/2014-5) and Coordenação de aperfeiçoamento de Pessoal de Nível Superior–Brasil (CAPES)–Finance Code 001.

**Institutional Review Board Statement:** The study was conducted according to the guidelines of the Declaration of Helsinki, and approved by the Institutional Review Board (or Ethics Committee) of the Universidade Federal de São Paulo (CEUA/UNIFESP 1907220814; August 27, 2014).

**Informed Consent Statement:** Not applicable.

**Data Availability Statement:** The data presented in this study are available on request from the corresponding author. The data are not publicly available due to privacy.

**Acknowledgments:** The authors thank Andre Aguilera, Marcia Araguth, Patricia Milanez and Ingrid Beatriz de Melo Morais for kind assistance in electron microscopy sample processing and figures format.

**Conflicts of Interest:** The authors declare no conflict of interest.

## References

- Goldberg, R.J. Tardive Dyskinesia in Elderly Patients. *J. Am. Med. Dir. Assoc.* **2003**, *4*, S32. [[CrossRef](#)]
- Morimoto, R.I.; Cuervo, A.M. Protein homeostasis and aging: Taking care of proteins from the cradle to the grave. *J. Gerontol. A Biol. Sci. Med. Sci.* **2009**, *64*, 167–170. [[CrossRef](#)]
- Ureshino, R.P.; Bertocini, C.R.; Fernandes, M.J.S.; Abdalla, F.M.F.; Porto, C.S.; Hsu, Y.T.; Lopes, G.S.; Smaili, S.S. Alterations in calcium signaling and a decrease in Bcl-2 expression: Possible correlation with apoptosis in aged striatum. *J. Neurosci. Res.* **2010**, *88*, 438–447. [[CrossRef](#)]
- Ureshino, R.P.; Hsu, Y.T.; do Carmo, L.G.; Yokomizo, C.H.; Nantes, I.L.; Smaili, S.S. Inhibition of cytoplasmic p53 differentially modulates Ca<sup>2+</sup> signaling and cellular viability in young and aged striata. *Exp. Gerontol.* **2014**, *58*, 120–127. [[CrossRef](#)]
- Terman, A. The effect of age on formation and elimination of autophagic vacuoles in mouse hepatocytes. *Gerontology* **1995**, *41*, 319–325. [[CrossRef](#)]
- Meléndez, A.; Tallóczy, Z.; Seaman, M.; Eskelinen, E.L.; Hall, D.H.; Levine, B. Autophagy genes are essential for dauer development and life-span extension in *C. elegans*. *Science* **2003**, *301*, 1387–1391. [[CrossRef](#)]
- Vicencio, J.M.; Galluzzi, L.; Tajeddine, N.; Ortiz, C.; Criollo, A.; Tasdemir, E.; Morselli, E.; Ben Younes, A.; Maiuri, M.C.; Lavandro, S.; et al. Senescence, apoptosis or autophagy? When a damaged cell must decide its path—A mini-review. *Gerontology* **2008**, *54*, 92–99. [[CrossRef](#)]
- Rubinsztein, D.C.; Mariño, G.; Kroemer, G. Autophagy and aging. *Cell* **2011**, *146*, 682–695. [[CrossRef](#)]
- Yang, Y.P.; Liang, Z.Q.; Gu, Z.L.; Qin, Z.H. Molecular mechanism and regulation of autophagy. *Acta Pharmacol. Sin.* **2005**, *26*, 1421–1434. [[CrossRef](#)]
- Kroemer, G.; Mariño, G.; Levine, B. Autophagy and the Integrated Stress Response. *Mol. Cell* **2010**, *40*, 280–293. [[CrossRef](#)]
- Yang, Z.; Klionsky, D.J. Eaten alive: A history of macroautophagy. *Nat. Cell Biol.* **2010**, *12*, 814–822. [[CrossRef](#)]
- Mizushima, N.; Komatsu, M. Autophagy: Renovation of cells and tissues. *Cell* **2011**, *147*, 728–741. [[CrossRef](#)]
- Ohsumi, Y. Molecular dissection of autophagy: Two ubiquitin-like systems. *Nat. Rev. Mol. Cell Biol.* **2001**, *2*, 211–216. [[CrossRef](#)]
- Mizushima, N. Autophagy: Process and function. *Genes Dev.* **2007**, *21*, 2861–2873. [[CrossRef](#)]
- Kurz, T.; Terman, A.; Gustafsson, B.; Brunk, U.T. Lysosomes and oxidative stress in aging and apoptosis. *Biochim. Biophys. Acta Gen. Subj.* **2008**, *1780*, 1291–1303. [[CrossRef](#)]
- Hara, T.; Nakamura, K.; Matsui, M.; Yamamoto, A.; Nakahara, Y.; Suzuki-Migishima, R.; Yokoyama, M.; Mishima, K.; Saito, I.; Okano, H.; et al. Suppression of basal autophagy in neural cells causes neurodegenerative disease in mice. *Nature* **2006**, *441*, 885–889. [[CrossRef](#)]
- Komatsu, M.; Waguri, S.; Chiba, T.; Murata, S.; Iwata, J.I.; Tanida, I.; Ueno, T.; Koike, M.; Uchiyama, Y.; Kominami, E.; et al. Loss of autophagy in the central nervous system causes neurodegeneration in mice. *Nature* **2006**, *441*, 880–884. [[CrossRef](#)]
- Rubinsztein, D.C. The roles of intracellular protein-degradation pathways in neurodegeneration. *Nature* **2006**, *443*, 780–786. [[CrossRef](#)]
- Williams, A.; Sarkar, S.; Cudston, P.; Ttofi, E.K.; Saiki, S.; Siddiqi, F.H.; Jahreiss, L.; Fleming, A.; Pask, D.; Goldsmith, P.; et al. Novel targets for Huntington's disease in an mTOR-independent autophagy pathway. *Nat. Chem. Biol.* **2008**, *4*, 295–305. [[CrossRef](#)]
- Sarkar, S.; Davies, J.E.; Huang, Z.; Tunnacliffe, A.; Rubinsztein, D.C. Trehalose, a novel mTOR-independent autophagy enhancer, accelerates the clearance of mutant huntingtin and  $\alpha$ -synuclein. *J. Biol. Chem.* **2007**, *282*, 5641–5652. [[CrossRef](#)]
- Harrison, D.E.; Strong, R.; Sharp, Z.D.; Nelson, J.F.; Astle, C.M.; Flurkey, K.; Nadon, N.L.; Wilkinson, J.E.; Frenkel, K.; Carter, C.S.; et al. Rapamycin fed late in life extends lifespan in genetically heterogeneous mice. *Nature* **2009**, *460*, 392–395. [[CrossRef](#)]
- Shaldubina, A.; Agam, G.; Belmaker, R.H. The mechanism of lithium action: State of the art, ten years later. *Prog. Neuropsychopharmacol. Biol. Psychiatry* **2001**, *25*, 855–866. [[CrossRef](#)]
- Crespo-Biel, N.; Camins, A.; Pallàs, M.; Canudas, A.M. Evidence of calpain/cdk5 pathway inhibition by lithium in 3-nitropropionic acid toxicity in vivo and in vitro. *Neuropharmacology* **2009**, *56*, 422–428. [[CrossRef](#)]
- Yasuda, S.; Liang, M.H.; Marinova, Z.; Yahyavi, A.; Chuang, D.M. The mood stabilizers lithium and valproate selectively activate the promoter IV of brain-derived neurotrophic factor in neurons. *Mol. Psychiatry* **2009**, *14*, 51–59. [[CrossRef](#)]
- Sugawara, H.; Sakamoto, K.; Harada, T.; Ishigooka, J. Predictors of efficacy in lithium augmentation for treatment-resistant depression. *J. Affect. Disord.* **2010**, *125*, 165–168. [[CrossRef](#)]
- Riadh, N.; Allagui, M.S.; Bourogaa, E.; Vincent, C.; Croute, F.; Elfeki, A. Neuroprotective and neurotrophic effects of long term lithium treatment in mouse brain. *BioMetals* **2011**, *24*, 747–757. [[CrossRef](#)]
- Sarkar, S.; Floto, R.A.; Berger, Z.; Imarisio, S.; Cordenier, A.; Pasco, M.; Cook, L.J.; Rubinsztein, D.C. Lithium induces autophagy by inhibiting inositol monophosphatase. *J. Cell Biol.* **2005**, *170*, 1101–1111. [[CrossRef](#)]
- Klein, P.S.; Melton, D.A. A molecular mechanism for the effect of lithium on development. *Proc. Natl. Acad. Sci. USA* **1996**, *93*, 8455–8459. [[CrossRef](#)]

29. Ryves, W.J.; Harwood, A.J. Lithium inhibits glycogen synthase kinase-3 by competition for magnesium. *Biochem. Biophys. Res. Commun.* **2001**, *280*, 720–725. [[CrossRef](#)]
30. Chalecka-Franaszek, E.; Chuang, D.M. Lithium activates the serine/threonine kinase Akt-1 and suppresses glutamate-induced inhibition of Akt-1 activity in neurons. *Proc. Natl. Acad. Sci. USA* **1999**, *96*, 8745–8750. [[CrossRef](#)]
31. Pan, J.Q.; Lewis, M.C.; Ketterman, J.K.; Clore, E.L.; Riley, M.; Richards, K.R.; Berry-Scott, E.; Liu, X.; Wagner, F.F.; Holson, E.B.; et al. AKT kinase activity is required for lithium to modulate mood-related behaviors in mice. *Neuropsychopharmacology* **2011**, *36*, 1397–1411. [[CrossRef](#)] [[PubMed](#)]
32. Sarkar, S.; Krishna, G.; Imarisio, S.; Saiki, S.; O’Kane, C.J.; Rubinsztein, D.C. A rational mechanism for combination treatment of Huntington’s disease using lithium and rapamycin. *Hum. Mol. Genet.* **2008**, *17*, 170–178. [[CrossRef](#)] [[PubMed](#)]
33. Liu, W.; Wang, Z.; Xia, Y.; Kuang, H.; Liu, S.; Li, L.; Tang, C.; Yin, D. The balance of apoptosis and autophagy via regulation of the AMPK signal pathway in aging rat striatum during regular aerobic exercise. *Exp. Gerontol.* **2019**, *124*, 110647. [[CrossRef](#)] [[PubMed](#)]
34. Liu, W.; Fu, R.; Wang, Z.; Liu, S.; Tang, C.; Li, L.; Yin, D. Regular Aerobic Exercise-Alleviated Dysregulation of CAMKII $\alpha$  Carbonylation to Mitigate Parkinsonism via Homeostasis of Apoptosis With Autophagy. *J. Neuropathol. Exp. Neurol.* **2020**, *79*, 46–61. [[CrossRef](#)]
35. Poulouse, S.M.; Bielinski, D.F.; Shukitt-Hale, B. Walnut diet reduces accumulation of polyubiquitinated proteins and inflammation in the brain of aged rats. *J. Nutr. Biochem.* **2013**, *24*, 912–919. [[CrossRef](#)]
36. Pereira, G.J.S.; Antonioli, M.; Hirata, H.; Ureshino, R.P.; Nascimento, A.R.; Bincoletto, C.; Vescovo, T.; Piacentini, M.; Fimia, G.M.; Smaili, S.S. Glutamate induces autophagy via the two-pore channels in neural cells. *Oncotarget* **2017**, *8*, 12730–12740. [[CrossRef](#)]
37. Klionsky, D.J.; Abdelmohsen, K.; Abe, A.; Abedin, M.J.; Abeliovich, H.; Arozena, A.A.; Adachi, H.; Adams, C.M.; Adams, P.D.; Adeli, K.; et al. Guidelines for the use and interpretation of assays for monitoring autophagy (3rd edition). *Autophagy* **2016**, *12*, 1–222. [[CrossRef](#)]
38. Fimia, G.M.; Stoykova, A.; Romagnoli, A.; Giunta, L.; Di Bartolomeo, S.; Nardacci, R.; Corazzari, M.; Fuoco, C.; Ucar, A.; Schwartz, P.; et al. Ambra1 regulates autophagy and development of the nervous system. *Nature* **2007**, *447*, 1121–1125. [[CrossRef](#)]
39. Ouimet, C.C.; Greengard, P. Distribution of DARPP-32 in the basal ganglia: An electron microscopic study. *J. Neurocytol.* **1990**, *19*, 39–52. [[CrossRef](#)]
40. Nonaka, S.; Chuang, D.M. Neuroprotective effects of chronic lithium on focal cerebral ischemia in rats. *Neuroreport* **1998**, *9*, 2081–2084. [[CrossRef](#)]
41. Wei, H.; Qin, Z.H.; Senatorov, V.V.; Wei, W.; Wang, Y.; Qian, Y.; Chuang, D.M. Lithium suppresses excitotoxicity-induced striatal lesions in a rat model of Huntington’s disease. *Neuroscience* **2001**, *106*, 603–612. [[CrossRef](#)]
42. Bianchi, P.; Ciani, E.; Contestabile, A.; Guidi, S.; Bartesaghi, R. Lithium restores neurogenesis in the subventricular zone of the ts65dn mouse, a model for down syndrome. *Brain Pathol.* **2010**, *20*, 106–118. [[CrossRef](#)] [[PubMed](#)]
43. Zhao, Q.; Liu, H.; Cheng, J.; Zhu, Y.; Xiao, Q.; Bai, Y.; Tao, J. Neuroprotective effects of lithium on a chronic MPTP mouse model of Parkinson’s disease via regulation of  $\alpha$ -synuclein methylation. *Mol. Med. Rep.* **2019**, *19*, 4989–4997. [[CrossRef](#)] [[PubMed](#)]
44. Carlson, S.W.; Dixon, C.E. Lithium improves dopamine neurotransmission and increases dopaminergic protein abundance in the striatum after traumatic brain injury. *J. Neurotrauma* **2018**, *35*, 2827–2836. [[CrossRef](#)] [[PubMed](#)]
45. Kim, Y.H.; Rane, A.; Lussier, S.; Andersen, J.K. Lithium protects against oxidative stress-mediated cell death in  $\alpha$ -synuclein-overexpressing in vitro and in vivo models of Parkinson’s disease. *J. Neurosci. Res.* **2011**, *89*, 1666–1675. [[CrossRef](#)]
46. Yu, F.; Wang, Z.; Tchanchou, F.; Chiu, C.T.; Zhang, Y.; Chuang, D.M. Lithium ameliorates neurodegeneration, suppresses neuroinflammation, and improves behavioral performance in a mouse model of traumatic brain injury. *J. Neurotrauma* **2012**, *29*, 362–374. [[CrossRef](#)]
47. Wix-Ramos, R.; Eblen-Zajjur, A. Time course of acute neuroprotective effects of lithium carbonate evaluated by brain impedance in the global ischemia model. *Can. J. Physiol. Pharmacol.* **2011**, *89*, 753–758. [[CrossRef](#)]
48. Chiu, C.T.; Liu, G.; Leeds, P.; Chuang, D.M. Combined treatment with the mood stabilizers lithium and valproate produces multiple beneficial effects in transgenic mouse models of huntington’s disease. *Neuropsychopharmacology* **2011**, *36*, 2406–2421. [[CrossRef](#)]
49. Cuervo, A.M. Autophagy and aging: Keeping that old broom working. *Trends Genet.* **2008**, *24*, 604–612. [[CrossRef](#)]
50. Yamamoto, T.; Takabatake, Y.; Kimura, T.; Takahashi, A.; Namba, T.; Matsuda, J.; Minami, S.; Kaimori, J.Y.; Matsui, I.; Kitamura, H.; et al. Time-dependent dysregulation of autophagy: Implications in aging and mitochondrial homeostasis in the kidney proximal tubule. *Autophagy* **2016**, *12*, 801–813. [[CrossRef](#)]
51. Azoulay-Alfaguter, I.; Elya, R.; Avrahami, L.; Katz, A.; Eldar-Finkelman, H. Combined regulation of mTORC1 and lysosomal acidification by GSK-3 suppresses autophagy and contributes to cancer cell growth. *Oncogene* **2015**, *34*, 4613–4623. [[CrossRef](#)] [[PubMed](#)]
52. Castillo-Quan, J.I.; Li, L.; Kinghorn, K.J.; Ivanov, D.K.; Tain, L.S.; Slack, C.; Kerr, F.; Nespital, T.; Thornton, J.; Hardy, J.; et al. Lithium Promotes Longevity through GSK3/NRF2-Dependent Hormesis. *Cell Rep.* **2016**, *15*, 638–650. [[CrossRef](#)] [[PubMed](#)]
53. Brunk, U.T.; Terman, A. Lipofuscin: Mechanisms of age-related accumulation and influence on cell function. *Free Radic. Biol. Med.* **2002**, *33*, 611–619. [[CrossRef](#)]
54. Mizushima, N.; Levine, B.; Cuervo, A.M.; Klionsky, D.J. Autophagy fights disease through cellular self-digestion. *Nature* **2008**, *451*, 1069–1075. [[CrossRef](#)] [[PubMed](#)]

55. O'Donovan, T.R.; Rajendran, S.; O'Reilly, S.; O'Sullivan, G.C.; McKenna, S.L. Lithium modulates autophagy in esophageal and colorectal cancer cells and enhances the efficacy of therapeutic agents in vitro and in vivo. *PLoS ONE* **2015**, *10*, e0134676. [[CrossRef](#)]
56. Fabrizi, C.; De Vito, S.; Somma, F.; Pompili, E.; Catizone, A.; Leone, S.; Lenzi, P.; Fornai, F.; Fumagalli, L. Lithium improves survival of PC12 pheochromocytoma cells in high-density cultures and after exposure to toxic compounds. *Int. J. Cell Biol.* **2014**. [[CrossRef](#)]
57. Fiorentini, A.; Rosi, M.C.; Grossi, C.; Luccarini, I.; Casamenti, F. Lithium improves hippocampal neurogenesis, neuropathology and cognitive functions in APP mice. *PLoS ONE* **2010**, *5*, e14382. [[CrossRef](#)]
58. Cui, J.; Shao, L.; Young, L.T.; Wang, J.F. Role of glutathione in neuroprotective effects of mood stabilizing drugs lithium and valproate. *Neuroscience* **2007**, *144*, 1447–1453. [[CrossRef](#)]
59. Shao, L.; Cui, J.; Young, L.T.; Wang, J.F. The effect of mood stabilizer lithium on expression and activity of glutathione s-transferase isoenzymes. *Neuroscience* **2008**, *151*, 518–524. [[CrossRef](#)]
60. Lin, M.T.; Beal, M.F. Mitochondrial dysfunction and oxidative stress in neurodegenerative diseases. *Nature* **2006**, *443*, 787–795. [[CrossRef](#)]
61. Navarro, A.; Boveris, A. Brain mitochondrial dysfunction in aging, neurodegeneration, and Parkinson's disease. *Front. Aging Neurosci.* **2010**, *2*, 34. [[CrossRef](#)] [[PubMed](#)]
62. Chen, J.F.; Liu, H.; Ni, H.F.; Lv, L.L.; Zhang, M.H.; Zhang, A.H.; Tang, R.N.; Chen, P.S.; Liu, B.C. Improved mitochondrial function underlies the protective effect of pirfenidone against tubulointerstitial fibrosis in 5/6 nephrectomized rats. *PLoS ONE* **2013**, *8*, e83593. [[CrossRef](#)] [[PubMed](#)]
63. Fornai, F.; Longone, P.; Cafaro, L.; Kastsuchenka, O.; Ferrucci, M.; Manca, M.L.; Lazzeri, G.; Spalloni, A.; Bellio, N.; Lenzi, P.; et al. Lithium delays progression of amyotrophic lateral sclerosis. *Proc. Natl. Acad. Sci. USA* **2008**, *105*, 2052–2057. [[CrossRef](#)] [[PubMed](#)]
64. Meyer, N.; Zielke, S.; Michaelis, J.B.; Linder, B.; Warnsmann, V.; Rakel, S.; Osiewacz, H.D.; Fulda, S.; Mittelbronn, M.; Münch, C.; et al. AT 101 induces early mitochondrial dysfunction and HMOX1 (heme oxygenase 1) to trigger mitophagic cell death in glioma cells. *Autophagy* **2018**, *14*, 1693–1709. [[CrossRef](#)] [[PubMed](#)]
65. Sheng, J.; Shen, L.; Sun, L.; Zhang, X.; Cui, R.; Wang, L. Inhibition of PI3K/mTOR increased the sensitivity of hepatocellular carcinoma cells to cisplatin via interference with mitochondrial-lysosomal crosstalk. *Cell Prolif.* **2019**, *52*, e12609. [[CrossRef](#)] [[PubMed](#)]
66. Thai, P.N.; Seidlmayer, L.K.; Miller, C.; Ferrero, M.; Dorn, G.W.; Schaefer, S.; Bers, D.M.; Dedkova, E.N. Mitochondrial quality control in aging and heart failure: Influence of ketone bodies and mitofusin-stabilizing peptides. *Front. Physiol.* **2019**, *10*, 382. [[CrossRef](#)] [[PubMed](#)]